PHYSICAL REVIEW B **72**, 201201(R) (2005)

Characterization of magnetic components in the diluted magnetic semiconductor $Zn_{1-x}Co_xO$ by x-ray magnetic circular dichroism

M. Kobayashi,[1] Y. Ishida,[1] J. l. Hwang,[1] T. Mizokawa,[1] A. Fujimori,[1] K. Mamiya,[2] J. Okamoto,[2] Y. Takeda,[2] T. Okane,[2] Y. Saitoh,[2] Y. Muramatsu,[2] A. Tanaka,[3] H. Saeki,[4] H. Tabata,[4] and T. Kawai[4]

[1]*Department of Physics and Department of Complexity Science and Engineering, University of Tokyo, Kashiwa, Chiba 277-8561, Japan*

[2]*Synchrotron Radiation Research Center, Japan Atomic Energy Research Institute, Mikazuki, Hyogo 679-5148, Japan*

[3]*Department of Quantum Matter, ADSM, Hiroshima University, Higashi-Hiroshima 739-8530, Japan*

[4]*Institute of Scientific and Industrial Research, Osaka University, Ibaraki, Osaka 567-0047, Japan*

(Received 2 September 2005; published 14 November 2005)

We report on the results of x-ray absorption, x-ray magnetic circular dichroism (XMCD), and photoemission experiments on $Zn_{1-x}Co_xO$ ($x=0.05$) thin film, which shows ferromagnetism at room temperature. The XMCD spectra show multiplet structures, characteristic of the Co^{2+} ion tetrahedrally coordinated by oxygen, suggesting that the ferromagnetism comes from Co ions substituting the Zn site in ZnO. The magnetic field and temperature dependences of the XMCD spectra imply that the nonferromagnetic Co ions are strongly coupled antiferromagnetically with each other.

DOI: 10.1103/PhysRevB.72.201201 PACS number(s): 75.50.Pp, 78.20.Ls, 78.70.Dm, 79.60.Dp

Diluted magnetic semiconductors (DMS's), in which a portion of atoms of the nonmagnetic semiconductor hosts are replaced by magnetic ions, are key materials for "spintronics" (spin electronics), which is intended to manipulate both the spin and charge degrees of freedom by use of coupling between the spins of the magnetic ions and the charge carriers of the host semiconductors.[1] However, because the Curie temperature (T_C) of the prototypical ferromagnetic DMS $Ga_{1-x}Mn_xAs$ is below the room temperature ($T_C<200$ K), it is still difficult to utilize DMS's in practical applications. Recently, oxide-based DMS's,[2] especially ZnO-based DMS's,[3–5] have attracted much attention as candidates for room temperature ferromagnetic DMS's. The wide band gap of ZnO is also expected to expand the range of applications. Theoretical studies have predicted that intrinsic ferromagnetism of Co-doped ZnO can be stabilized by electron doping.[6,7] However, possible extrinsic origins of the ferromagnetism such as precipitated Co metal clusters[8] have not been excluded and the ferromagnetism of $Zn_{1-x}Co_xO$ is still in strong dispute.

Although magnetization measurements and anomalous Hall effect measurements are suitable to investigate magnetic properties, it is not straightforward to judge from these measurements whether the ferromagnetism is intrinsic or extrinsic.[9] X-ray magnetic circular dichroism (XMCD), which is the difference in core-level absorption spectra between right- and left-handed circularly polarized x rays, is an element specific probe sensitive to the magnetic polarization of each element, and therefore enables us to directly extract the local electronic structure related to particular magnetic properties of the substituted transition-metal ions.[10,11] In this work, we have performed combined x-ray absorption (XAS), XMCD and photoemission spectroscopy (PES) studies of $Zn_{1-x}Co_xO$ to determine the electronic structure and the magnetic properties associated with the Co ions. In particular, the XMCD line shape and the intensity under varying magnetic field (H) and temperature (T) have implied that the ferromagnetism of $Zn_{1-x}Co_xO$ is indeed caused by the Co^{2+} ions substituting the Zn site.

A $Zn_{1-x}Co_xO$ ($x=0.05$) thin film was epitaxially grown on an α-Al_2O_3 (0001) substrate by the pulsed laser deposition technique using an ArF excimer laser with energy density 1.0 J/cm^2. During the deposition, the substrate was kept at a temperature of $\sim$300 °C in an oxygen pressure of 1.0×10^{-5} mbar. The total thickness of the $Zn_{1-x}Co_xO$ layer was $\sim$2000 Å on a 500 Å ZnO buffer layer. X-ray diffraction confirmed that the thin film had the wurtzite structure and no secondary phase was observed. Details of the sample fabrication are given in Ref. 12. The film does not contain Al as a dopant unlike Ref. 3. Ferromagnetism with T_C above the room temperature was confirmed by magnetization measurements using a SQUID magnetometer (Quantum Design, Co. Ltd.).

XAS and XMCD measurements at the Co $2p\rightarrow3d$ (Co $L_{2,3}$) edge were performed at beamline BL23SU[13] of SPring-8 in the total-electron yield mode. The monochromator resolution was $E/\Delta E>10\,000$. Right-handed (μ^+) and left-handed (μ^-) circularly polarized x-ray absorption spectra were obtained by reversing photon helicity at each photon energy. The degree of circular polarization of the x rays is expected to be over 90%. External magnetic field was applied perpendicular to the sample surface. In all the experiment, we measured μ^+ and μ^- spectra by changing the polarization and averaging μ^+ and μ^- between the opposite field direction. The background of the XAS spectra was assumed to be a hyperbolic tangent function as usual. Circularly polarized x-ray absorption spectra under each experimental condition have been normalized to the maximum height of the Co $L_{2,3}$ edge XAS $[(\mu^++\mu^-)/2]$ spectra as 100. Ultraviolet photoemission (UPS) measurements were performed at BL-18A of Photon Factory (PF), High Energy Accelerator Research Organization (KEK). Spectra were taken at room temperature in a vacuum below 7.5×10^{-10} Torr. The total resolution of the spectrometer (VG CLAM hemispherical analyzer) including temperature broadening was $\sim$200 meV. X-ray photoemission (XPS) measurements were performed using a Gammadata Scienta SES-100 hemispheri-

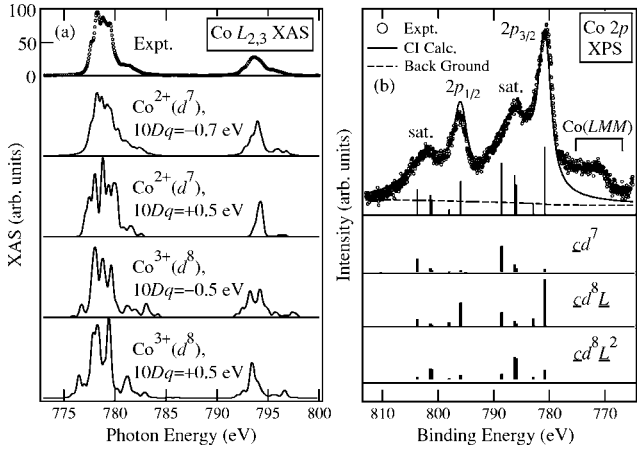

FIG. 1. Co 2p core-level spectra of $Zn_{0.95}Co_{0.05}O$. (a) Experimental Co $L_{2,3}$ edge XAS spectrum (top) compared with atomic multiplet calculations, in which the Co valence and the sign and magnitude of the crystal-field 10Dq are varied. The positive and negative 10Dq mean that the Co ion is coordinated octahedrally and tetrahedrally by oxygen atoms. (b) Co 2p XPS spectrum and CI cluster-model analysis. $\underline{c}$ and $\underline{L}$ denote a hole in the Co 2p and the ligand 2p orbitals, respectively.

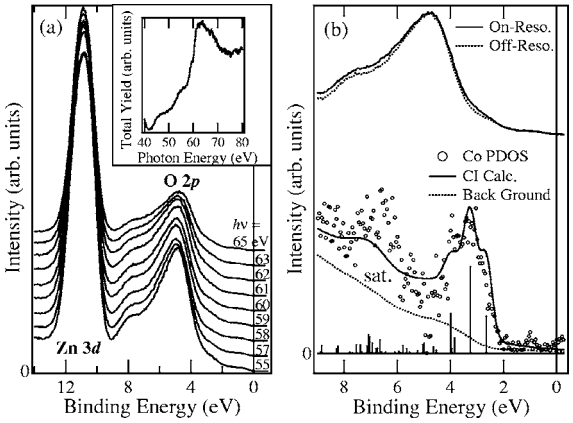

FIG. 2. Valence-band UPS spectra of $Zn_{0.95}Co_{0.05}O$. (a) A series of photoemission spectra for photon energies in the Co $3p \rightarrow 3d$ core-excitation region. Inset: Absorption spectrum recorded in the total electron yield mode. (b) Top: On-resonance ($h\nu$=61.5 eV) and off-resonance ($h\nu$=60.0 eV) spectra. The difference between these spectra represents the Co 3d PDOS. Bottom: CI cluster-model analysis for the Co 3d PDOS.

cal analyzer and an Al $K\alpha$ source ($h\nu$=1486.6 eV) in a vacuum below 1.0×10^{-9} Torr. In both UPS and XPS measurements, photoelectrons were collected in the angle integrated mode. Sample surface was cleaned by cycles of Ar^+-ion sputtering at 1.5 kV and annealing at 250 °C. Cleanliness of the sample surface was checked by the absence of a high binding-energy shoulder in the O 1s spectrum and C 1s contamination by XPS.

Figure 1(a) shows the Co $L_{2,3}$ XAS spectrum compared with spectra calculated using atomic multiplet theory. The calculation was carried out for Co^{2+} and Co^{3+} with the positive and negative crystal-field parameter 10Dq representing the octahedral and tetrahedral coordinations of oxygen atoms for Co, respectively. The calculated multiplet splitting for Co^{3+} is more spread than experiment both for the octahedral and tetrahedral crystal fields, and the calculated spectra for Co^{2+} better reproduce the experiment. Furthermore, the negative 10Dq better reproduces the measured XAS spectrum. Hence, we conclude that the Co ion is divalent and is tetrahedrally coordinated by four oxygen atoms.

Further information about the local electronic structure of the Co^{2+} ion, namely, hybridization of the Co 3d orbital with the host oxygen 2p orbital as well as the d-d Coulomb interaction can be studied by photoemission spectroscopy.[14,15] The Co core-level 2p XPS spectrum of $Zn_{0.95}Co_{0.05}O$ shown in Fig. 1(b) is similar to that of CoO.[16] We have made a configuration-interaction (CI) cluster-model analysis of the Co 2p XPS spectrum using a $[Co^{2+}(O^{2-})_4]^{6-}$ cluster and estimated the electronic structure parameters: the ligand-to-3d charge-transfer energy Δ=5.0±0.5 eV, the d-d Coulomb interaction energy U=6.0±0.5 eV, and the Slater-Koster parameter $(pd\sigma)$=−1.6±0.1 eV. These parameters are in good agreement with those obtained from the previous XAS study[17] and are consistent with the chemical trend in transition-metal-doped II-VI DMS's.[18] Here, Racah parameters have been fixed at the values of the free ion: B=0.138 eV and C=0.54 eV. The Co 3d-2p core hole Coulomb attraction energy Q is related to U through $U=\beta Q$, where at β=0.7. The ratio between $(pd\sigma)$ and $(pd\pi)$ has been fixed $(pd\sigma)/(pd\pi)$=−2.16. Figure 1(b) shows that the main peak of the spectrum dominantly consists of charge-transferred states, i.e., $\underline{c}d^8\underline{L}$, where $\underline{c}$ and $\underline{L}$ denote a hole in the Co 2p and oxygen 2p orbitals, respectively.

Figure 2(a) shows the valence-band UPS spectra of $Zn_{0.95}Co_{0.05}O$ taken at various photon energies in the Co $3p \rightarrow 3d$ core-excitation region. The absorption spectrum in the same energy region is shown in the inset. Binding energies (E_B's) are referenced to the Fermi level (E_F) of a metallic sample holder which is in electrical contact with the sample. The absorption spectrum shows that Co $3p \rightarrow 3d$ absorption occurs at $h\nu \sim 61$ eV. Constant-initial-state (CIS) spectra at various E_B's (not shown) indicate that the Co 3d partial density of states (PDOS) is primarily located at $E_B \sim 3.0$ and ~7.0 eV. Figure 2(b) shows the Co 3d PDOS of $Zn_{0.95}Co_{0.05}O$, which has been obtained by subtracting the off-resonance ($h\nu$=60 eV) spectrum from the on-resonance ($h\nu$=61.5 eV) one. Here, the off-resonance spectrum was multiplied by the integrated $(0<E_B<9$ eV) intensity ratio between $h\nu$=61.5 and 60 eV of pure ZnO. The Co 3d PDOS shows a peak at $E_B \sim 3.0$ eV, which is similar to that of the polycrystalline $Zn_{0.9}Co_{0.1}O$,[19] and a satellite at $E_B \sim 7.0$ eV. Because the energy difference between the top of the O 2p band and E_F is nearly equal to the band gap of ZnO, E_F is supposed to be located near the conduction band minimum (composed of Zn 4s and possibly of Co d states), meaning that the sample is n-type. Although local-density approximation (LDA) calculations have predicted that ferromagnetism is mediated by carriers and therefore needs a high density of states (DOS) at E_F,[6] we could not clearly observe a finite DOS at E_F, consistent with the low carrier density. The energy difference between the main structure and the satellite of the Co 3d PDOS was as large ~9 eV for CoO,[16] while it

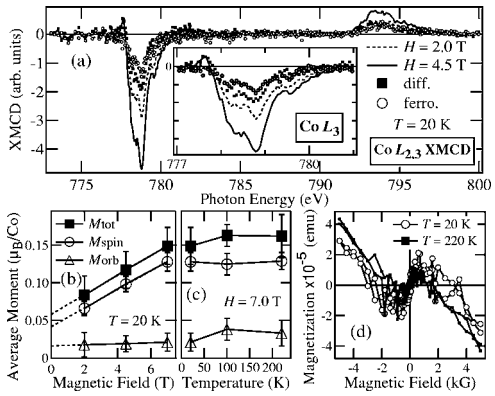

FIG. 3. Magnetic field and temperature dependences of the Co $L_{2,3}$ XMCD spectra of $Zn_{0.95}Co_{0.05}O$. (a) XMCD spectra under different magnetic fields at 20 K. Closed circle shows the difference of the spectra between $H=4.5$ and 2.0 T. Open circle shows the ferromagnetic component. (b) Average magnetic moments M_{spin}, M_{orb}, and M_{tot} as functions of magnetic field, estimated using the XMCD sum rules. (c) The same as (b) as function of temperature. (d) Magnetization curves measured by a SQUID magnetometer.

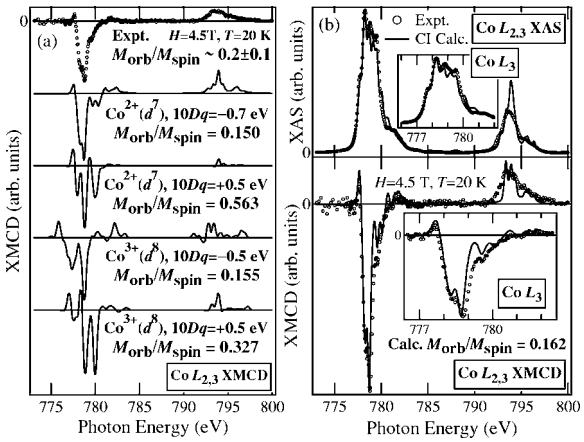

FIG. 4. Co $L_{2,3}$ XMCD spectra of $Zn_{0.95}Co_{0.05}O$. (a) Comparison with atomic multiplet calculation, in which the valence of Co and the sign and magnitude of the crystal-field splitting are varied. (b) CI cluster-model analysis for the XAS and XMCD spectra.

is ~4 eV for $Zn_{1-x}Co_xO$, probably because of the different coordinations of oxygen atoms between CoO and $Zn_{1-x}Co_xO$. This can be well explained by the CI cluster-model calculation using the same Δ, U, $(pd\sigma)$ as shown in Fig. 2(b).

Although the XAS spectra were nearly independent of the magnetic field and μ^+ and μ^- were nearly identical on the scale of Fig. 1(a), there were weak but reproducible XMCD signals $(\mu^+-\mu^-)$ as shown in Fig. 3(a). The intensity of XMCD spectra increases with increasing magnetic field as shown in Fig. 3(b), while it is rather independent of temperature as shown in Fig. 3(c). Note that, in Figs. 3(b) and 3(c), the spin (M_{spin}), orbital (M_{orb}), and total (M_{tot}) magnetic moments of Co estimated using XMCD sum rules[20,21] are plotted rather than the raw XMCD intensities. Part of the XMCD signals which linearly increases with H represents the paramagnetic component, while XMCD signals which persist at $H\sim 0$ T represent the ferromagnetic component.[22] The difference between the XMCD spectra at $H=2.0$ and 4.5 T reflects the paramagnetic component as shown in Fig. 3(a). The ferromagnetic component obtained by subtracting the appropriate paramagnetic component from the XMCD spectrum at $H=2.0$ T is shown in Fig. 3(a). The line shape of the ferromagnetic component is nearly identical to that of the paramagnetic spectrum. Therefore, it seems that the Co ions have similar electronic structures in the paramagnetic and the ferromagnetic components. It should be emphasized that the XMCD spectra also show a multiplet structure, unlike those of Co metal,[23] indicating that, though only a part of the doped transition-metal ions are ferromagnetic,[11] the magnetism in the present sample is not due to metallic Co clusters but due to Co ions with localized 3d electrons. Figure 3(d) shows the magnetization curves measured by a SQUID magnetometer. The saturation magnetization estimated from the XMCD intensity is somewhat smaller than that measured by the SQUID magnetometer. It is possible that there is a magnetic dead layer near the surface region.

As in the case of the XAS spectrum, the XMCD spectra are also compared with theoretical XMCD spectra calculated using atomic multiplet theory as shown in Fig. 4(a). The calculated ratio M_{orb}/M_{spin} is compared with experiment. The line shape of the calculated spectra for Co^{3+} are different from the experimental one and that for Co^{2+} with tetrahedral oxygen coordination best agrees with experiment. Comparison of the ratio M_{orb}/M_{spin} between the calculated spectra and experiment indicates that the Co^{2+} ion with tetrahedral oxygen coordination and not octahedral one is consistent with experiment. Therefore, the calculated spectrum for Co^{2+} with $10Dq=-0.7$ eV best reproduces the experimental XMCD. To examine more details of the XAS and XMCD line shapes, CI cluster-model calculations were performed as shown in Fig. 4(b). We have used electronic structure parameters $\Delta=5.0$ eV, $U=5.0$ eV, and $(pd\sigma)=-1.6$ eV, nearly the same as those estimated from the PES experiments. The calculated M_{orb}/M_{spin} is closer to the experimental value than that of atomic multiplet theory. This gives further support that the substituted Co ions under tetrahedral crystal field are responsible for the ferromagnetism in $Zn_{1-x}Co_xO$.

Finally we comment on possible origins of the temperature-independent paramagnetic component of the XMCD signals. This signal cannot be due to Pauli paramagnetism of conduction electrons because their XMCD spectra show characteristic of the Co^{2+} ion and also that its susceptibility $\chi_{exp}\sim 1.43\times 10^{-2}$ (μ_B/T per Co) is several orders of magnitude larger than the Pauli paramagnetism expected for the conduction electron concentration $n\sim 1.0\times 10^{17}$ cm^{-3} of the present sample. If the temperature-independent paramagnetism is due to the Co^{2+} ions, there should be strong antiferromagnetic interaction between the Co ions because, if the Co ions do not interact with each other, they would show the Curie behavior. The temperature-independent paramagnetic component may arise from the susceptibility of the antiferromagnetic Co ions having a Néel temperature above the room temperature. Such magnetic susceptibility is estimated to be $g^2S(S+1)/T_N\sim 8.4\times 10^{-3}$ (μ_B/T per Co) for $g=2$, $S=3/2$, and $T_N=400$ K, in reasonable agreement with slope of

the XMCD intensity [Fig. 3(b)] of $\chi_{exp} \sim 1.43 \times 10^{-2}$ (μ_B/T per Co). Although both the ferromagnetic and paramagnetic/antiferromagnetic Co ions has the same 2+ valence and the tetrahedral crystal field, subtle differences such as the kind of the nearest neighbor cation (Zn or Co), neighboring defects, and local lattice distortion may have lead to the different magnetic behaviors. In particular, the formation of ferromagnetic Co-rich regions cannot be excluded. In order to confirm the above conjectures, more precise and systematic XMCD measurements on samples with varying Co and carrier concentrations are necessary.

In summary, we have performed XAS, XMCD, and PES experiments on the diluted ferromagnetic semiconductor *n*-type $Zn_{1-x}Co_xO$ ($x=0.05$). The XMCD spectra show a multiplet structure, characteristic of the Co^{2+} ion tetrahedrally coordinated by oxygen. This implies that the ferromagnetism in $Zn_{1-x}Co_xO$ is caused by the substituted Co^{2+} ions at the Zn site. The magnetic field and temperature dependences of the XMCD intensity suggest that the nonferromagnetic Co ions are strongly coupled antiferromagnetically with each other.

We thank T. Okuda, A. Harasawa, and T. Kinoshita for technical help at PF. We also thank the Materials Design and Characterization Laboratory, Institute for Solid State Physics, University of Tokyo, for the use of the SQUID magnetometer. This work was supported by a Grant-in-Aid for Scientific Research in Priority Area "Semiconductor Nanospintronics" (14076209) from the Ministry of Education, Culture, Sports, Science and Technology, Japan. The experiment at PF was approved by the Photon Factory Program Advisory Committee (Proposal No. 2002G027). M.K. acknowledges support from the Japan Society for the Promotion of Science for Young Scientists.

[1] H. Ohno, F. Matsukura, and Y. Ohno, Japan Society of Applied Physics International **5**, 4 (2002).
[2] S. J. Pearton, W. H. Heo, M. Ivill, D. P. Norton, and T. Steiner, Semicond. Sci. Technol. **19**, R59 (2004).
[3] K. Ueda, H. Tabata, and T. Kawai, Appl. Phys. Lett. **79**, 988 (2001).
[4] H. Saeki, H. Tabata, and T. Kawai, Solid State Commun. **120**, 439 (2001).
[5] P. Sharma, A. Gupta, K. V. Rao, F. J. Owens, R. Sharma, R. Ahuja, J. M. O. Guillen, B. Johanssion, and G. A. Gehring, Nat. Mater. **2**, 673 (2003).
[6] K. Sato and H. Katayama-Yoshida, Jpn. J. Appl. Phys., Part 1 **40**, L334 (2001).
[7] E.-C. Lee and K. J. Chang, Phys. Rev. B **69**, 085205 (2004).
[8] J.-Y. Kim, J.-H. Park, B.-G. Park, H.-J. Noh, S.-J. Oh, J. S. Yang, D.-H. Kim, S. D. Bu, T.-W. Noh, H.-J. Lin, H.-H. Hsieh, and C. T. Chen, Phys. Rev. Lett. **90**, 017401 (2003).
[9] S. R. Shinde, S. B. Ogale, J. S. Higgins, H. Zheng, A. J. Millis, V. N. Kulkarni, R. Ramesh, R. L. Greene, and T. Venkatesan, Phys. Rev. Lett. **92**, 166601 (2004).
[10] D. J. Keavney, D. Wu, J. W. Freeland, E. Johnston-Halperin, D. D. Awschalom, and J. Shi, Phys. Rev. Lett. **91**, 187203 (2003).
[11] H. Ohldag, V. Solinus, F. U. Hillebrecht, J. B. Goedkoop, M. Finazzi, F. Matsukura, and H. Ohno, Appl. Phys. Lett. **76**, 2928 (2000).
[12] H. Saeki, H. Matsui, T. Kawai, and H. Tabata, J. Phys.: Condens. Matter **16**, S5533 (2004).
[13] J. Okamoto, K. Mamiya, S.-I. Fujimori, T. Okane, Y. Saitoh, Y. Muramatsu, A. Fujimori, S. Ishikawa, and M. Takano, AIP Conf. Proc. **705**, 1110 (2004).
[14] J. Okabayashi, A. Kimura, O. Rader, T. Mizokawa, A. Fujimori, T. Hayashi, and M. Tanaka, Phys. Rev. B **58**, R4211 (1998).
[15] J. Okabayashi, A. Kimura, T. Mizokawa, A. Fujimori, T. Hayashi, and M. Tanaka, Phys. Rev. B **59**, R2486 (1999).
[16] Z.-X. Shen, J. W. Allen, P. A. P. Lindberg, D. S. Dessau, B. O. Wells, A. Borg, W. Ellis, J. S. Kang, S. J. Oh, I. Lindau, and W. E. Spicer, Phys. Rev. B **42**, 1817 (1990).
[17] J. Okabayashi, K. Ono, M. Mizuguchi, M. Oshima, S. S. Gupta, D. D. Sarma, T. Mizokawa, A. Fujimori, M. Yuri, C. T. Chen, T. Fukumura, M. Kawasaki, and H. Koinuma, J. Appl. Phys. **95**, 3573 (2004).
[18] T. Mizokawa and A. Fujimori, Phys. Rev. B **56**, 6669 (1997).
[19] S. C. Wi, J.-S. Kang, J. H. Kim, S.-B. Cho, B. J. Kim, S. Yoon, B. J. Suh, S. W. Han, K. H. Kim, K. J. Kim, B. S. Kim, H. J. Song, H. J. Shin, J. H. Shim, and B. I. Min, Appl. Phys. Lett. **84**, 4233 (2004).
[20] B. T. Thole, P. Carra, F. Sette, and G. van der Laan, Phys. Rev. Lett. **68**, 1943 (1992).
[21] P. Carra, B. T. Thole, M. Altarelli, and X. Wang, Phys. Rev. Lett. **70**, 694 (1993).
[22] A. Fujimori, J. Okabayashi, Y. Takeda, T. Mizokawa, J. Okamoto, K. Mamiya, Y. Saitoh, Y. Muramatsu, M. Oshima, S. Ohya, and M. Tanaka, J. Electron Spectrosc. Relat. Phenom. **144–147**, 701 (2005).
[23] C. T. Chen, Y. U. Idzerda, H.-J. Lin, N. V. Smith, G. Meigs, E. Chaban, G. H. Ho, E. Pellegrin, and F. Sette, Phys. Rev. Lett. **75**, 152 (1995).